Hyperspectral eye fundus imaging with extended spectral range towards the near infrared

T. Alterini, F. Díaz-Doutón, M. Vilaseca

T. Alterini, F. Díaz-Doutón, M. Vilaseca, "Hyperspectral eye fundus imaging with extended spectral range towards the near infrared," Proc. SPIE 11073, Clinical and Preclinical Optical Diagnostics II, 110730Y (19 July 2019); doi: 10.1117/12.2523453

SPIE.

Event: European Conferences on Biomedical Optics, 2019, Munich, Germany

Hyperspectral eye fundus imaging with extended spectral range towards the near infrared

Alterini T.[*] [a], Díaz-Doutón F.[a], Vilaseca M.[a]
[a] Centre de Desenvolupament de Sensors, Instrumentació i Sistemes (CD6), Universitat Politècnica de Catalunya, Rambla de Sant Nebridi 10, 08222 Terrassa, Barcelona, Spain

ABSTRACT

Eye fundus photography routinely used in clinical practice is restricted to color imaging of the retina. In the last years, hyperspectral imaging has shown to be a powerful tool for the spectral analysis of biological tissue. In this study, we present a fully custom-made fast hyperspectral fundus camera based on light emitting diodes (LED) with 15 different wavelengths of emission and with extended spectral sensitivity towards the near infrared (NIR) (from 400 nm to 1300 nm), which allows imaging deeper retinal layers, including the choroid, than current clinical devices. These new features will be very useful for a better understanding of ocular diseases as well as aiding in their diagnosis.

Keywords: Hyperspectral imaging, fundus camera, retina, LED

1. INTRODUCTION

The increase of life expectancy experienced in the last decades and the improved health policies are being translated into a growth of the aging population worldwide, which is well known to have higher risk of eye disorders. Thus, new systems able to contribute to the non-invasive and objective diagnosis of ocular diseases are demanded. In particular, as many important eye and systemic diseases early manifest themselves in the retina, acquiring good quality images of the ocular fundus has been traditionally a matter of especial relevance. Fundus photography is nowadays one of the most used clinical tools for retinal screening and early detection of pathologies. Current commercial fundus cameras use color imaging sensors, being therefore restricted to only three spectral bands (RGB images). Moreover, due to metamerism, many structures might remain hidden. Hyperspectral imaging technology has recently come into view as a promising and powerful tool for the spectral analysis of living tissues. In the case of eye fundus photography, it can potentially increase the amount of extractable information, highlighting particular retinal structures or the presence of certain biological substances due to their different spectral reflectance. In this regard, several works have already been carried out, focused in characterizing the dynamics and shape of several structures, such as retinal metabolism and/or vessels, drusen etc.[1-3]. However, due to the relatively complex optical design of fundus cameras, these works made use of modified commercial instruments, which are mainly restricted to the visible (VIS) range of the spectrum (400 nm to 700 nm)[4]. Accordingly, the aim of this work was the development of a novel hyperspectral fundus camera based on LED illumination allowing the fast imaging of the retina not only in the visible but also in the near infrared (NIR) region of the electromagnetic spectrum - through 15 spectral bands (from 400 nm to 1300 nm) -, which has never been explored in fundus photography. In this work, we present the custom-made set-up, as well as its characterization, that has been designed and implemented in order to image the ocular fundus in such a broad spectral range. Preliminary in-lab test results in living eyes are also shown.

2. EXPERIMENTAL SET-UP

The fundus camera prototype was designed and optimized by means of optical simulation software (Zemax, Radiant Zemax). Custom illumination and detection strategies were conceptualized with the focus set on achieving, through the whole working wavelength range, the best illumination and light collection efficiency, aberration balance and cost (only commercial optical components used). It was finally implemented in a preclinical prototype (see Figure 1).

The system schematically consists of one illumination arm and two detection arms: one for the spectral range between 400 nm to 950 nm (VIS-NIR1 detection arm), and another for 960 nm to 1300 nm (NIR2 detection arm). They all share the objective lens, which is placed in front of the patient's eye. Regarding the illumination, the used light source consists of

[*] tommaso.alterini@upc.edu; phone +34 634677727; www.cd6.upc.edu

Clinical and Preclinical Optical Diagnostics II, edited by J. Quincy Brown, Ton G. van Leeuwen,
Proc. of SPIE-OSA, SPIE Vol. 11073, 110730Y · © 2019 SPIE-OSA
CCC code: 1605-7422/19/$21 · doi: 10.1117/12.2523453

15 LEDs clusters (peaks wavelengths at 416 nm, 450 nm, 471 nm, 494 nm, 524 nm, 595 nm, 598 nm, 624 nm, 660 nm, 732 nm, 865 nm, 955 nm, 1025 nm, 1096 nm, 1213 nm), welded on 3 different printed boards. In each board, LEDs are arranged in a ring-shaped configuration. In particular the so called VIS ring comprises LEDs with peak wavelengths from 400 nm to 660 nm, the NIR1 from 732 nm to 1096 nm and the NIR 2 is composed by 4 LEDs emitting at 1213 nm. To ensure the optical separation between the back reflected illumination light from the patient's optical elements, such as the cornea and crystalline lens, an image of these rings is resembled on a 45° custom-made holed mirror, conjugated with the patient's pupil plane. This mirror couples the illumination (reflected) and detection paths (transmitted through the mirror's central hole), assessing the geometrical pupil separation of both paths required to avoid the presence of reflections of the ring-shaped illumination from the cornea and the crystalline lens in the acquired images[4].

The wavelengths of the LEDs were chosen in order to obtain as much information as possible from the light absorption and reflection on the structures and typical substances present in the ocular fundus[2,3]. The light from different rings is then combined in a common optical path by means of two dichroic mirrors with cut-off wavelengths at 1150 nm and 700 nm. In the detection paths, after the holed mirror and the objective, a properly designed set of lenses is placed in order to image the retina on the camera's sensors, correct for aberrations and compensate for patient's spherical refraction (range: ± 15 D). The split of the VIS-NIR1 and the NIR2 detection paths is achieved with a dichroic mirror with a cut-off wavelength at 950 nm. The used camera sensors were a CMOS detector (Orca Flash 4.0, Hamamatsu, Japan) and an InGaAs camera (C12741-03, Hamamatsu, Japan) for the VIR-NIR1 and NIR2 detection arms, respectively. Finally, a fixation target is placed at a retinal conjugate plane in the illumination arm to allow patients' fixation while performing the measurements. The electronics required for the control of the illumination and detection systems was also developed. The LEDs emission and the cameras acquisition are synchronized by means of trigger signals, allowing the sequential recording of the whole set of 15 spectral images in 613 ms, from NIR to VIS wavelengths. A user-friendly MATLAB interface was developed for the precise control of the system's operation and parameters setting.

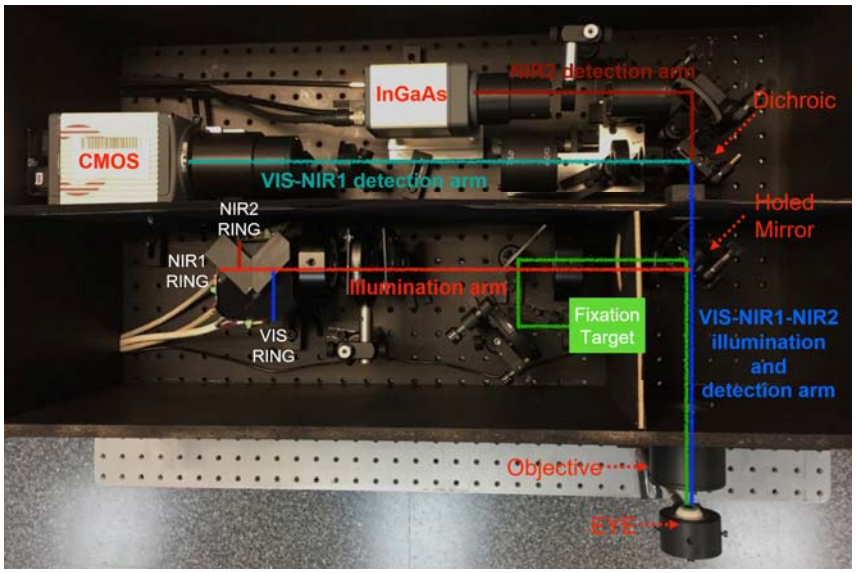

Figure 1. Schematic top-view of the experimental set-up.

3. RESULTS

3.1 Optical characterization of the system

The prototype was characterized following the ISO standards for ophthalmic instruments and fundus cameras (ISO 15004-2:2007[5] and ISO 10940:2009[6]), including the two detection arms of the system with CMOS and InGaAs cameras, respectively. We measured the resolving power of the system, the angular field of view (FOV) and the magnification (M) (see Table 1). The resulting system has an angular field of view of 30° approximately, and a resolution below the limit imposed by the used imaging sensors.

Table 1. Field of view (FOV) and magnification (M) measured following the ISO standards. The resolving power of the system, i. e., the minimum separation allowing recognition of two adjacent lines on the fundus expressed as number of line pairs per millimeter (lp/mm), is given for the central, medium ($> r/2, \leq r$) and peripheral FOV ($> r$) ($2r$ is the total diameter of the circular FOV).

Detection arm (camera)	FOV ± ΔFOV (°)	M ± ΔM	Central FOV (lp/mm)	Medium FOV (lp/mm)	Peripheral FOV (lp/mm)
VIS-NIR1 (CMOS)	30.4 ± 0.2	1.20 ± 0.2	60	40	20
NIR2 (InGaAs)	31.1 ± 0.3	0.88 ± 0.05	25	25	13

3.2 Spectral and radiometric characterization of the system

In order to characterize our system in terms of emitted radiation, we carried out measurements of radiometric power (W) and irradiance (W/m^2). The normalized spectral distribution of each LED at the pupil plane, where the illumination light is focused, was also analyzed. A power meter PM100D (Thorlabs Inc., New Jersey, United States) equipped with a photodiode sensor S120C (Thorlabs Inc., New Jersey, United States) with sensitivity between 400 nm and 1100 nm was used to perform measurements of absolute radiometric power (W). A scanning spectrometer Spectro 320 from Instrument Systems (Instrument Systems GmbH, München, Germany) with sensitivity between 370 nm and 1700 nm attached to the accessory EOP-146 allowed spectral irradiance measurements of the light incident to the module. The spectral radiometric power of each LED and the corresponding peak wavelength and full width at half maximum (FWHM) are shown in Table 2.

Table 2. Peak wavelength, full width at half maximum (FWHM) and radiometric power of the LEDs of the system.

Peak wavelength (nm)	*FWHM ± ΔFWHM (nm)*	$RP_{100\%} \pm \Delta RP_{100\%}$ *(mW)*
416	16 ± 2	2.35 ± 0.04
450	18 ± 2	2.5 ± 0.2
471	27 ± 3	3.40 ± 0.07
494	31 ± 3	2.18 ± 0.09
525	33 ± 3	1.91 ± 0.03
595	17 ± 2	0.13 ± 0.01
598	76 ± 5	2.25 ± 0.02
624	17 ± 2	0.98 ± 0.06
660	19 ± 2	2.47 ± 0.07
732	29 ± 3	1.82 ± 0.04
865	37 ± 3	4.0 ± 0.3
955	58 ± 4	6.4 ± 0.5
1025	44 ± 4	0.55 ± 0.01
1096	97 ± 5	0.086 ± 0.005
1213	77 ± 5	0.54 ± 0.03

3.3 System repeatability

The stability of the system was ensured by means of an analysis of its repeatability. In particular, the repeatability of the system was tested by performing the same measurement along different days (mid-term repeatability) and taking the measurements consecutively (short-term repeatability). We used an artificial eye (OEMI-7, Ocular instrument Inc., Washington, United States) to perform the measurements to avoid including the instability given by the patient. For each measurement, two streams of images were acquired, one with the LED at the 100% of its maximum emission and another with the LED at 0%. This is necessary to ensure a good background subtraction and to keep the measure independent from the ambient light. For the mid-term repeatability, we took a total of 10 measurements in 5 consecutive days (early in the morning and late in the afternoon). In order to have an estimation of the repeatability, the averaged intensity on the same portion of the image was calculated for all wavelengths and for all measurements. Once we finished with the mid-term repeatability, the short-term repeatability was analyzed. Specifically, we acquired 10 complete streams of images consecutively. The images were then analyzed as in the mid-term study. The results obtained are shown in Figure 2. As it

can be seen, the percentage of variation of both the mid- and the short-term analysis were lower that 2.98 % and 1.98 %, respectively.

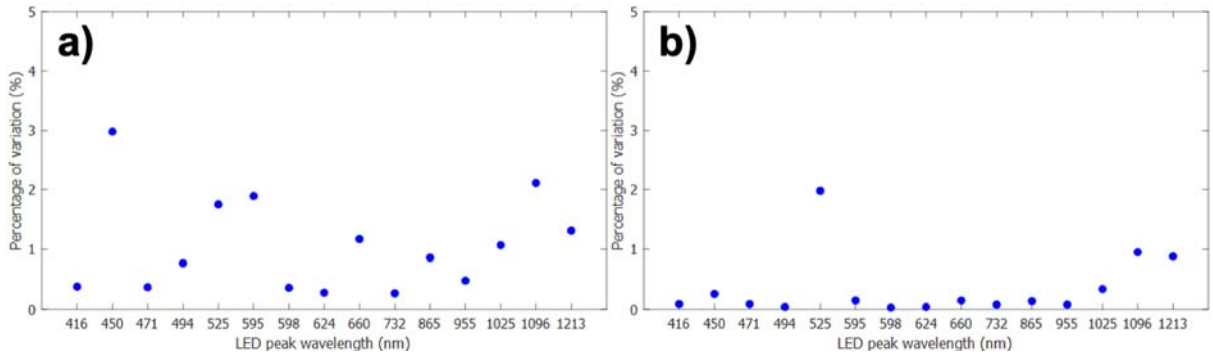

Figure 2. Mid-term (a) and short-term (b) percentage of variability calculated dividing the standard deviation by the averaged intensity value of the same portion of the image.

3.4 Safety evaluation

The evaluation of the light hazard protection followed the ISO 10940[5], which is guide for the measurements and the calculations of the relative values for the light hazard for fundus camera systems. This standard refers to the more general one ISO 15004-2:2007[6], which is also considered here and includes recommendations for ophthalmic instruments in general. This standard classifies ophthalmic instruments into either Group 1 or Group 2 in order to distinguish instruments that are non-hazardous from those that are potentially hazardous.

For the hyperspectral system (pulsed light source), the following quantities were measured (in J/cm^2):

- H_{VIR-R}: R(λ) weighted retinal visible and infrared radiation radiant exposure
- H_{IR-CL}: unweighted corneal and lenticular infrared radiation radiant exposure
- H_{VIR-AS}: unweighted anterior segment visible and infrared radiation radiant exposure

All quantities were below the safety limits established by the standards, so that the hyperspectral fundus camera could be classified as Group 1.

3.5 Multispectral fundus images

Measurements with the hyperspectral fundus camera were carried out in a small group of volunteers in a laboratory environment, as a first and preclinical evaluation of the system's performance (Figure 3). As expected, short wavelengths such as blue and green are reflected and scattered back more superficially, so that structures as the optic disk, nerve fibers, and retinal blood vessels are well contrasted in images corresponding to this spectral region. On the contrary, for wavelengths in the NIR range, especially those longer than 950 nm, information from layers beyond the retina such as the choroid is available due to the reduced absorption of tissue chromophores and thus, deeper penetration of light. It is worth noting the contrast differences between retinal veins and arteries and the surrounding fundus, which are noticeable if one compares the images from 500 nm to 700 nm, mainly due to the different spectral absorption of oxygenated and de-oxygenated hemoglobin. It is also remarkable that the image at 416 nm is of poorer quality, mainly due to low retinal reflectance and preceding transmission of the ocular media.

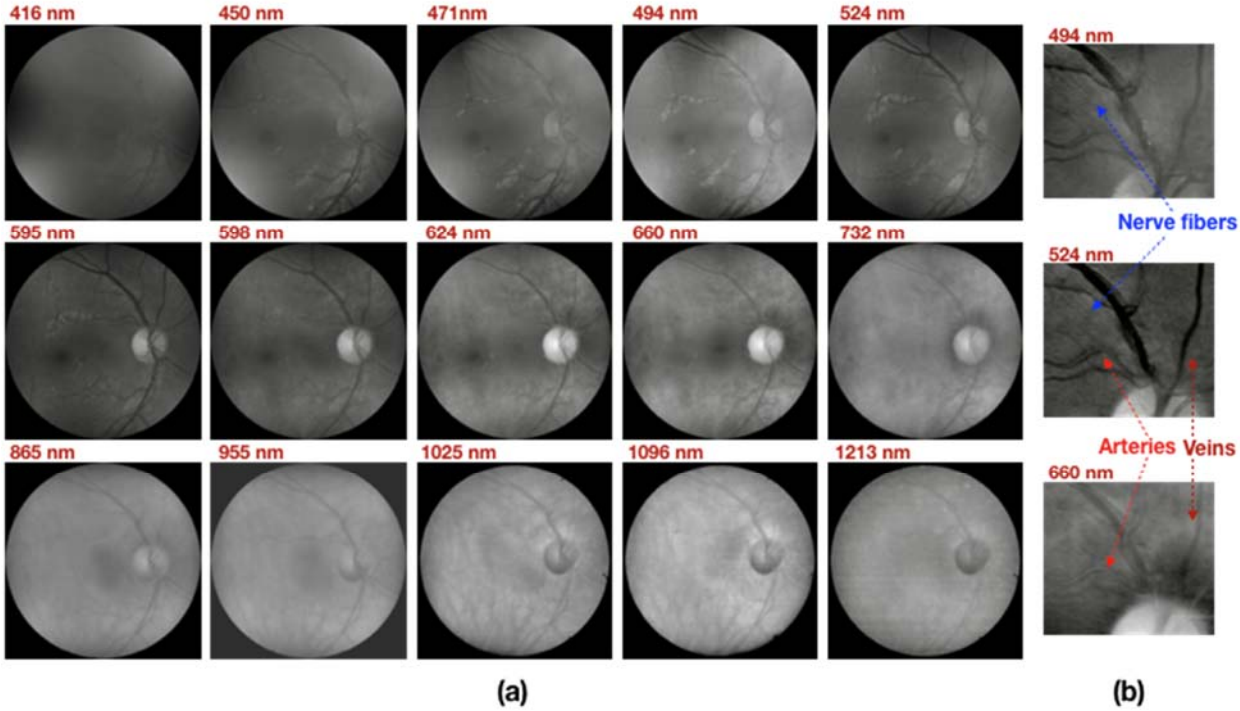

Figure 3. Sequence of hyperspectral images acquired with the fundus camera (a) and details of nerve fibers, arteries and veins (b).

4. CONCLUSIONS AND FUTURE WORK

The ocular fundus extended hyperspectral analysis that can be performed with the developed system permit the assessment of retinal structures from an unprecedented point of view. These capabilities may be relevant for the early diagnosis of retinal diseases such as glaucoma, age related macular degeneration, melanomas, neurofibromatosis, etc. A first clinical validation of this prototype is planned in a short term, where the hyperspectral images from a set of patients suffering from the abovementioned diseases will be measured and compared with healthy eyes.

5. ACKNOWLEDGEMENTS

This work was supported by the European Union through the project Advanced BiomEdical OPTICAL Imaging and Data Analysis (BE-OPTICAL) under Grant 675512.

REFERENCES

[1] Lu, G. and Fei, B., "Medical hyperspectral imaging: a review," *J. Biomed. Opt.*, vol. 19, no. 1, p. 23 (2014).
[2] Berendschot, T. J., DeLintb, M., P. J. and Norren, D. V, "Fundus reflectance—historical and present ideas," *Prog. Retin. Eye Res.*, vol. 22, no. 2, pp. 171–200 (2003).
[3] Mordant, D.J., Al-abboud, I, Muyo, G., Gorman, A., Harvey, A.R. and McNaugth, A.I., "Spectral imaging of the retina," *Eye (Lond).*, vol. 25, no. 3, pp. 309–20 (2011).
[4] Kaschke, M., K., Donnerhacke, H. and Rill, M. S., [Optical Devices in Ophthalmology and Optometry: Technology, Design Principles and Clinical Applications], Wiley-VCH Verlag GmbH & Co. KGaA, Weinheim, (2014).
[5] ISO 15004-2:2007. Ophthalmic instruments — Fundamental requirements and test methods — Part 2: Light hazard protection. International Organization for Standardization.
[6] ISO 10940:2009. Ophthalmic instruments -- Fundus cameras. International Organization for Standardization.